3D Face Recognition using Patch Geodesic Derivative Pattern

Soheila Gheisari[1], Shahram Javadi[2], and Alireza Kashaninya[3]

[1,2,3] Electrical Engineering Department, Central Tehran Branch, Islamic Azad University, Tehran, Iran
s.gheisari@iauctb.ac.ir, sh.javadi@iauctb.ac.ir, ali.kashaniniya@iauctb.ac.ir

Abstract

In this paper, a novel Patch Geodesic Derivative Pattern (PGDP) describing the texture map of a face through its shape data is proposed. Geodesic adjusted textures are encoded into derivative patterns for similarity measurement between two 3D images with different pose and expression variations. An extensive experimental investigation is conducted using the publicly available Bosphorus and BU-3DFE databases covering face recognition under pose and expression changes. The performance of the proposed method is compared with the performance of the state-of-the-art benchmark approaches. The encouraging experimental results demonstrate that the proposed method is a new solution for 3D face recognition in single model databases.

Keywords: 3D Face, Geodesic Distance, Derivative

1. Introduction

Face recognition has been used vastly in security systems and Human Computer Interaction (HCI). Because the human face is a three dimensional object, using the 3D images can improve the performance of the face recognition algorithms. While most efforts have been devoted to face recognition from the range maps of the 3D images, a few approaches have utilized both range and texture maps.

Cartoux et al. [1] used facial profiles extracted from range images for face recognition. Gordon [2]suggested the feature extraction based on depth and curvature features. Tanaka et al. [3] used the surface curvature information of a 3D shape for face recognition. Chua et al. [4] extended the use of point signature to recognize frontal face scans with expression changes. Hesher et al. [5] applied PCA to the range images, and estimated the coefficients' probability. Pan et al. [6] used the partial directed Housdorff distance to match two range images. Chang et al. [7] showed that the face recognition performances on texture and depth images are same. However, their combination improves the recognition rate. Lu et al. [8] used a matching algorithm between 2.5D face images and 3D face models for face recognition under pose variations. They used a modified ICP algorithm to match an input 2.5D image and the reference 3D models. Bronstein et al. [9] proposed an expression-invariant representation of faces called "canonical image" by calculating the geodesic distances between points on the face surface. Mian et al. [10] used Scale-Invariant Feature Transform (SIFT) descriptor accompanying with the 3D spherical face representation to overcome the face recognition under facial expression changes. Malassiotis and Strintzis [11] proposed a technique for face recognition using the range map to compensate pose variations in the texture map using the ICP algorithm. They used an Embedded Hidden Markov Model (EHMM) [12] as the classifier. Hajati et al. [13] recently proposed the Patch Geodesic Moments (PGMs) using Zernike moments controlled by the geodesic distances of the

face points which are robust to expression and pose changes.

In this paper, we present a novel 3D face recognition approach using derivative patterns controlled by the geodesic shape information to tackle the problem of face recognition under pose and expression variations from one exemplar per person. To have a texture representation based on the shape information, we use the geodesic distance to control the texture descriptor function. The feasibility and effectiveness of the proposed method is investigated using the publically available Bosphorus [14] and BU-3DFE [15] databases which contain faces under different pose and expression changes. The recognition rate of the system is compared with the recognition rate of the state-of-the-art approaches. Our encouraging experimental results demonstrate that the proposed method is a novel solution for pose and expression-invariant face recognition using 3D images.

This paper is organized as follows: Section 2 describes Patch Geodesic Derivative Pattern (PGDP) concept in detail. A feasibility investigation and performance evaluation of the proposed approach is given in Section 3. Finally, the paper concludes in Section 4.

2. Method

The scheme of the proposed method is illustrated in Fig.1. In this method, the corresponding texture map is created from an input 3D image. In the next step, the texture map is transformed to a transformed texture map based on the geodesic distances of the face points. Then, the transformed texture map is partitioned into equal-sized square patches and a derivative descriptor is applied to each patch. By concatenating the feature vector of all patches, a feature vector for the subject is created. Finally, the input subject is identified by computing the dissimilarity between the query and all models in the gallery. The algorithm will be described in the following subsections.

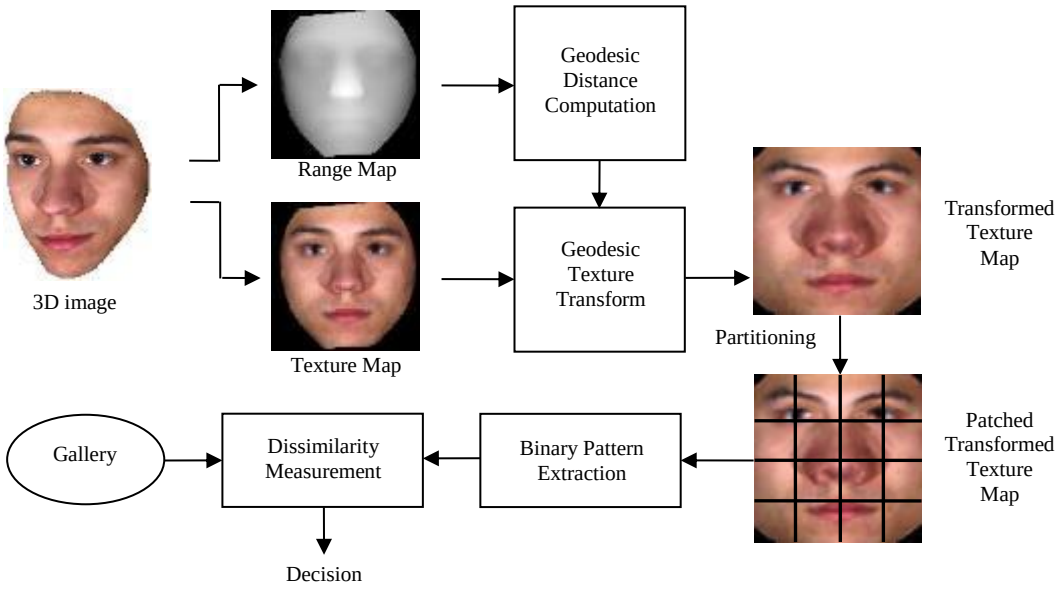

Fig.1. The scheme of the proposed method

2.1. Geodesic Texture Transform

In this paper, we use the face isometric assumption to establish a texture transform which is pose-invariant. We represent the texture map of a 3D image as $f^t(x,y)$. For each pixel in the texture map, we have a geodesic distance from the nose tip computed using the 3D image. The transform of the point $Q(x,y)$ in the texture map is computed as

$$F^t(x_{trans}, y_{trans}) = f^t(x,y) \quad (1)$$

where

$$x_{trans} = r(x,y)\cos\big(\varphi(x,y)\big) + 80 \quad (2)$$

and

$$y_{trans} = r(x,y)\sin\big(\varphi(x,y)\big) + 70 \quad (3)$$

where $F^t(x_{trans}, y_{trans})$denotes the transformed texture map. x_{trans} and y_{trans} are the coordinates of the transformed texture map. $r(x,y)$ is the geodesic distance of the point $Q(x,y)$ from the nose tip.

In (2) and (3), $\varphi(x,y)$ is the angle made by the connecting line of $Q(x,y)$and the nose tip $P(x_{nose}, y_{nose})$ as well as the horizon line in the texture map computed as follows:

$$\varphi(x,y)=\begin{cases}0, & x=x_{nose}, y=y_{nose}\\ \tan^{-1}\left(\frac{y-y_{nose}}{x-x_{nose}}\right), & x\geq x_{nose}\\ \tan^{-1}\left(\frac{y-y_{nose}}{x-x_{nose}}\right)+\pi, & x<x_{nose}\end{cases} \quad (4)$$

2.2. Patch Derivative Pattern

In this section, we first partition the transformed texture map to equal-sized square patches in a non-overlapping way. Given a $N\times N$ transformed texture map and $W\times W$ patches, we indicate all points in a patch with p and q indexes which are integers ranging from 1 to N/W as

$$p=\lfloor x_{trans}/W\rfloor+1\ ;\ 0\leq x_{trans}<N \quad (5)$$

$$q=\lfloor y_{trans}/W\rfloor+1\ ;\ 0\leq y_{trans}<N \quad (6)$$

which x_{trans} and $y_{trans}$are the coordinates of the transformed texture map. In (5) and (6), the symbol $\lfloor\cdot\rfloor$ represents the floor function.

Given a transformed texture map $F^t(x_{trans},y_{trans})$, the (p,q)th patch in the transformed texture map $F^t_{p,q}(x^{pq},y^{pq})$ is defined as

$$F^t_{p,q}(x^{pq},y^{pq})=F^t(W(p-1)+x^{pq},W(q-1)+y^{pq}) \quad (7)$$

where x^{pq} and y^{pq} are coordinates of the (p,q)th patch.

Given the (p,q)th patch in the transformed texture map, $F^t_{p,q}(x^{pq},y^{pq})$, the derivatives along 0°, 45°, 90° and 135° directions are denoted as $F'^t_{p,q(\alpha)}(x^{pq},y^{pq})$ where α = 0°, 45° , 90° and 135°. Let (x_0^{pq},y_0^{pq}) be a point in $F^t_{p,q}(x^{pq},y^{pq})$, and (x_i^{pq},y_i^{pq}), $i=1,2,\dots,8$ be the neighboring points around (x_0^{pq},y_0^{pq}) (see Fig.2). The four first-order derivatives at (x_0^{pq},y_0^{pq}) can be written as

$$F'^t_{p,q(0)}(x_0^{pq},y_0^{pq})=F^t_{p,q}(x_0^{pq},y_0^{pq})-F^t_{p,q}(x_5^{pq},y_5^{pq}) \quad (8)$$

$$F'^t_{p,q(45)}(x_0^{pq},y_0^{pq})=F^t_{p,q}(x_0^{pq},y_0^{pq})-F^t_{p,q}(x_3^{pq},y_3^{pq}) \quad (9)$$

$$F'^t_{p,q(90)}(x_0^{pq},y_0^{pq})=F^t_{p,q}(x_0^{pq},y_0^{pq})-F^t_{p,q}(x_2^{pq},y_2^{pq}) \quad (10)$$

$$F'^t_{p,q(135)}(x_0^{pq},y_0^{pq})=F^t_{p,q}(x_0^{pq},y_0^{pq})-F^t_{p,q}(x_1^{pq},y_1^{pq}) \quad (11)$$

Patch Geodesic Derivative Pattern for the (p,q)th patch in α direction at (x_0^{pq},y_0^{pq}), $PGDP_{p,q\,(\alpha)}\left(F^t_{p,q}(x_0^{pq},y_0^{pq})\right)$, is defined as

$$PGDP_{p,q\,(\alpha)}\left(F^t_{p,q}(x_0^{pq},y_0^{pq})\right)=\left\{f\left(F'^t_{p,q(\alpha)}(x_0^{pq},y_0^{pq}),F'^t_{p,q(\alpha)}(x_1^{pq},y_1^{pq})\right),\ f\left(F'^t_{p,q(\alpha)}(x_0^{pq},y_0^{pq}),F'^t_{p,q(\alpha)}(x_2^{pq},y_2^{pq})\right),\ \dots,f\left(F'^t_{p,q(\alpha)}(x_0^{pq},y_0^{pq}),F'^t_{p,q(\alpha)}(x_8^{pq},y_8^{pq})\right)\right\} \quad (12)$$

(x_1^{pq},y_1^{pq})	(x_2^{pq},y_2^{pq})	(x_3^{pq},y_3^{pq})
(x_4^{pq},y_4^{pq})	(x_0^{pq},y_0^{pq})	(x_5^{pq},y_5^{pq})
(x_6^{pq},y_6^{pq})	(x_7^{pq},y_7^{pq})	(x_8^{pq},y_8^{pq})

Fig.2. An 8-neighborhood around (x_0^{pq},y_0^{pq})

where

$$f\left(F'^t_{p,q(\alpha)}(x_0^{pq},y_0^{pq}),F'^t_{p,q(\alpha)}(x_i^{pq},y_i^{pq})\right)=\begin{cases}0, & if\ F'^t_{p,q(\alpha)}(x_0^{pq},y_0^{pq}).F'^t_{p,q(\alpha)}(x_i^{pq},y_i^{pq})>0\\ 1, & if\ F'^t_{p,q(\alpha)}(x_0^{pq},y_0^{pq}).F'^t_{p,q(\alpha)}(x_i^{pq},y_i^{pq})\leq 0\end{cases} \quad (13)$$

The binary Patch Geodesic Derivative Pattern for the (p,q)th patch,$PGDP_{p,q}\left(F^t_{p,q}(x^{pq},y^{pq})\right)$, is defined as the concatenation of the four 8-bit directional PGDPs:

$$PGDP_{p,q}\left(F^t_{p,q}(x^{pq},y^{pq})\right)=\left\{PGDP_{p,q\,(\alpha)}\left(F^t_{p,q}(x^{pq},y^{pq})\right)|\alpha=0°,45°,90°,135°\right\} \quad (14)$$

Then, the binary patch geodesic derivative pattern is converted into the corresponding decimal value as

$$DPGDP_{p,q}\left(F^t_{p,q}(x^{pq},y^{pq})\right)=\sum_{k=1}^{32}2^{k-1}\cdot PGDP^{(k)}_{p,q}\left(F^t_{p,q}(x^{pq},y^{pq})\right) \quad (15)$$

where $PGDP^{(k)}_{p,q}\left(F^t_{p,q}(x^{pq},y^{pq})\right)$ denotes the k-th bit of the binary patch geodesic derivative pattern.

We model the distribution of $DPGDP$s using the spatial histogram as

$$HPGDP_{p,q}\left(F^t_{p,q}(x^{pq},y^{pq})\right)=H\left\{DPGDP_{p,q}\left(F^t_{p,q}(x^{pq},y^{pq})\right)\right\} \quad (16)$$

Finally, we concatenate the histograms of the patches to build a feature vector for the subject

$$HPGDP(f^t(x,y)) = \left\{HPGDP_{p,q}\left(F^t_{p,q}(x^{pq},y^{pq})\right)|p,q = 1,\dots,N/W\right\} \quad (17)$$

For a given query 3D image, we compute its feature distance against all model 3D images in the gallery. The model in the gallery with the minimum distance is considered as the correct match.

3. Results

In order to evaluate the performance of the proposed algorithm, an extensive experimental investigation is conducted, covering face recognition under different pose and expression variations. For pose variation, the experiments were conducted on the Bosphorus database [14] which contains 3D face scans of 105 subjects with different pose variations. Fig. 3 illustrates different pose rotations in the database. In the pre-processing step, the original transformed texture maps were cropped to the size of 160×160 pixels in the way that the distance of the nose tip is 80 pixels from the sides, 90 and 70 pixels from the top and the bottom, respectively. We use the Euclidean distance for dissimilarity measuring between subjects.

First, the parameter of the algorithm (i.e. the size of the patches W) is chosen using a training dataset which is selected randomly from the Bosphorus database [14]. The rank-1 recognition rate of the proposed algorithm has been measured using the training dataset for W=160, 80, 40, 32, 20, 16, 10, 8, and 4. The result is illustrated in Fig. 4. As can be seen, the best performance of the algorithm is occurred when W=8. Thus, we select W=8 in the next experiments.

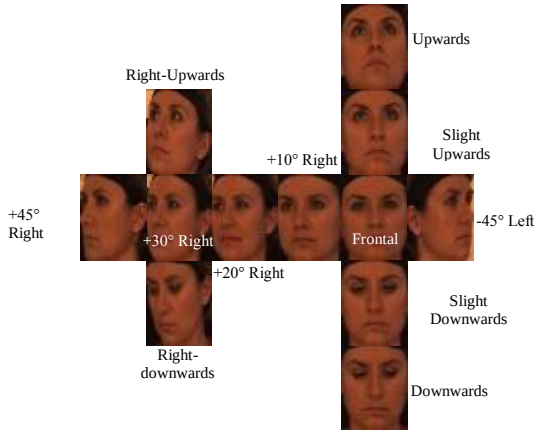

Fig.3. Different types of rotations in the Bosphorus face database [14]

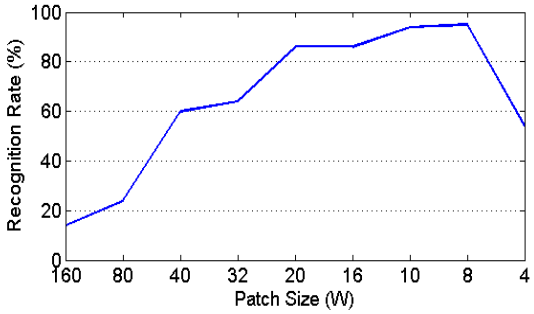

Fig.4. Recognition rate versus patch size (W)

Second, the performance of the proposed method in all pose rotations is compared with three benchmark approaches: 1) the method of Malassiotis and Strintzis [11] for pose-invariant 3D face recognition, 2) Local Binary Pattern (LBP) [16] applied directly on the texture map, and 3) Patch Geodesic Moments [13] for 3D face recognition. The rank-1 recognition rates of the methods are tabulated in Table 1. In all experiments, we build a gallery from the frontal faces, while the rotated faces are used as the probe. The proposed method has 96.1% recognition rate in +10° right rotation, while the benchmarks have the recognition rate of 65.7%, 95.2%, and 92.3%, respectively. In +20° right rotation, the recognition rate is 91.4%, 52.4%, 83.8%, and 88.6% for the proposed method and three benchmarks, respectively. Finally, in +30° right rotation, the recognition rate is 80.1%, 42.9%, 67.6%, 80% for the proposed method and three benchmarks, respectively. The overall recognition rate of the proposed method is much higher than the recognition rate of the benchmarks (71.4% compared with 50%, 61%, and 69.1%).

Table 1.
The rank-1 recognition rates (%) for different methods

Rotation Considered	Malassiotis and Strintzis [11]	LBP [16]	PGM [13]	PGDP
+10° Right	65.7	95.2	92.3	96.1
+20° Right	52.4	83.8	88.6	91.4
+30° Right	42.9	67.6	80	80.1
+45° Right	9.5	17.1	39	36.2
-45° Left	21	13.3	38.1	37.1
Upwards	69.5	79	79	91.4
Slight Upwards	81.9	90.5	87.6	96.2
Slight Downwards	84.8	85.7	87.6	86.7
Downwards	68.6	62.9	69.5	70
Right-Upwards	31.4	52.4	63.8	64.7
Right-Downwards	21.9	23.8	34.3	35.2
Overall	**50**	**61**	**69.1**	**71.4**

To evaluate the performance of the proposed algorithm under the expression changes the BU-3DFE dataset [15], one of the important dataset for face recognition under expression variations, has been used. This dataset includes 3D scans with

relating texture of 56 women and 44 men (totally 100 people) in various expressions. Each person has totally 25 scans containing of one neutral and six kinds of expressions. Fig. 5 illustrates these expressions which include anger, happiness, sadness, surprise, disgust, and fear in four different intensities.

To test the algorithm on BU-3DFE dataset, we divided scans of each person into two sets of "low intensity" and "high intensity". Low intensity set contains of 1200 scans with low intensity expressions and high intensity set contains of other 1200 scans with high intensity expressions. Note that neutral scans are not considered. We choose "low intensity versus high intensity" and "high intensity versus low intensity" scenarios for classification. In the first scenario, the low intensity set is the train set and the high intensity set is the test set, and vice versa [17]. The rank-1 recognition rate for each expression of anger, happiness, sadness, surprise, disgust, and fear is provided in Table 2. This parameter in all expressions with both strategies is higher than 95%. In addition the open mouth problem in some expressions like surprise that decreases recognition rate in many other methods has been solved.

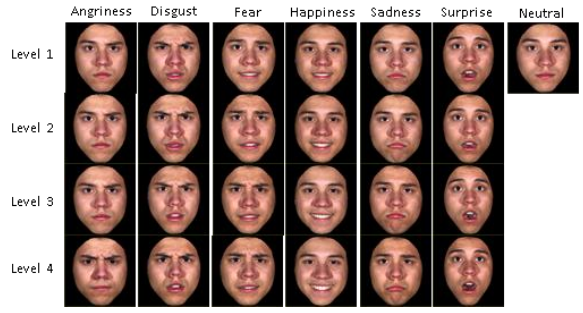

Fig.5. An example set of faces for one subject in the BU-3DFE database.

Table 2.
The rank-1 recognition rate of the proposed method under different expressions.

Expression	Rank-1 recognition rate (%)	
	Low int. vs. high int.	High int. vs. low int.
Angry	96	98.5
Disgust	95	99
Fear	97.5	99.5
Happy	99	99
Sad	98.5	99.5
Surprise	96.5	99

Comparison results between our approach and the benchmark methods are present in Table 3. Despite we have used all six expressions and more probe images, we achieved better performance than Smeet et al. [18]. Also, with approximately same number of probe images we achieved higher recognition rate compared to Mpiperis et al. [19]. Kaushik et al. [20] reported above 98% recognition rate which seems is better than our result, but they have used the limited number of probes. Furthermore, our results are similar to Lei et al. [17].

Table.3.
Comparison of the rank-1 recognition rate under expression changes.

Method	No. of probes	R-1 recognition rate (%)
The proposed Method	1200	98.1
Smeets et al. [18]	900	89.9
Mpiperis et al. [19]	1250	86
Kaushik et al. [20]	695	98.9
Lei et al. [17]	1200	98.2

4. Conclusion

In this paper, a novel 3D face recognition method has been proposed called Patch Geodesic Derivative Pattern (PGDP). PGDP is designed to handle the variations in the face surface due to the pose and expression changes. Based on the geodesic distance between face surface points, a new technique to transform the texture map of the 3D model and to extract patterns is proposed. The patch derivative patterns controlled by geodesic distance are used in the proposed face recognition approach as local descriptors. It is very encouraging to find that the performance of the proposed method under the pose variations is much higher compared with that of three state-of-the-art benchmarks under the pose variations (overall recognition rate of 71.4% compared with 50%, 61%, and 69.1%). Moreover, the proposed method has improved the recognition rate by 4.8% under expression changes compared to the average recognition rate of the benchmarks.

References

[1] J. Y. Cartoux, J. T. Lapreste, M. Richetin, Face Authentication or Recognition by Profile Extraction from Range Images, Proc. of the Workshop Interpretation of 3D Scenes, pp.194-199, 1989.

[2] G. G. Gordon, Face Recognition Based on Depth and Curvature Features, Proc. of the IEEE Conference on Computer Vision and Pattern Recognition, pp.108-110, 1992.

[3] H. T. Tanaka, M. Ikeda, H. Chiaki, Curvature-Based Face Surface Recognition Using Spherical Correlation-Principal Directions for Curved Object Recognition, Proc. of the 3rd. IEEE International Conference on Face and Gesture Recognition, pp.372-377, 1998.

[4] C. Chua, F. Han, Y. Ho, 3D Human Face Recognition Using Point Signature, Proc. of the 4th IEEE International Conference on Automatic Face and Gesture Recognition, pp.233-238, 2000.

[5] C. Hesher, A. Srivastava, G. Erlebacher, Principal Component Analysis of Range Images for Facial Recognition, Proc. of the International Conference on Imaging Science, Systems, and Technology, pp.62-68, 2002.

[6] G. Pan, Z. Wu, Y. Pan, Automatic 3D Face Verification from Range Data, Proc. of the IEEE International Conference on Acoustics, Speech, and Signal Processing, pp.193-196, 2003.

[7] S. D. Chang, M. Rioux, J. Domey, Face recognition with range images and intensity images, Optical Engineering, Vol.36, No.4, pp.1106-1112, 1997.

[8] X. Lu, A. K. Jain, D. Colbry, Matching 2.5D Face Scans to 3D Models, IEEE Trans. on Pattern Analysis and Machine Intelligence, Vol.28, No.1, pp.31-43, 2006.

[9] A. M. Bronstein, M. M. Bronstein, R. Kimmel, Expression-Invariant Representations of Faces, IEEE Trans. on Image Processing, Vol.16, No.1, pp.188-197, 2007.

[10] A. S. Mian, M. Bennamoun, R. Owens, An efficient multimodal 2D-3D hybrid approach to automatic face recognition, IEEE Trans. on Pattern Analysis and Machine Intelligence, Vol.29, No.11, pp.1927-1943, 2007.

[11] S. Malassiotis, M. G. Strintzis, Robust Face Recognition Using 2D and 3D Data: Pose and Illumination Compensation, Pattern Recognition, Vol.38, No.12, pp.2537-2548, 2005.

[12] L. R. Rabiner, Tutorial on Hidden Markov Models and Selected Applications in Speech Recognition, Proc. IEEE, Vol.77, No.2, pp.257-286, 1989.

[13] F. Hajati, A. A. Raie, Y. Gao, 2.5D Face Recognition using Patched Geodesic Moments, Pattern Recognition, Vol.45, No.3, pp.969-982, 2012.

[14] A. Savran, N. Alyuz, H. Dibeklioglu, O. Celiktutan, B. Gokberk, B. Sankur, L. Akarun, Bosphorus Database for 3D Face Analysis, Proc. of the First COST 2101 Workshop on Biometrics and Identity Management (BIOID), pp.47-56, 2008.

[15] L. Yin, X. Wei, Y. Sun, J. Wang, M. J. Rosato, A 3D Facial Expression Database for Facial Behavior Research, Proc. of the 7th International Conference on Automatic Face and Gesture Recognition (FGR), pp.211-216, 2006.

[16] T. Ahonen, A. Hadid, M. Pietikainen, Face Description with Local Binary Patterns: Application to Face Recognition, IEEE Trans. on Pattern Analysis and Machine Intelligence, Vol.28, No.12, pp.2037-2041, 2006.

[17] Y. Lei, M. Bennamoun, A. A. El-Sallam, An efficient 3D face recognition approach based on the fusion of novel local low-level features, Pattern Recognition, Vol.46, No.1, pp.24-37, 2013.

[18] D. Smeets, T. Fabry, J. Hermans, D. Vandermeulen, P. Suetens, Fusion of an Isometric Deformation Modeling Approach Using Spectral Decomposition and a Region-Based Approach Using ICP for Expression-Invariant 3D Face Recognition, Proceedings of the 2010 20th International Conference on Pattern Recognition, pp.1172-1175, 2010.

[19] I. Mpiperis, S. Malassiotis, M. G. Strintzis, Expression-Compensated 3D Face Recognition with Geodesically Aligned Bilinear Models, Biometrics: Theory, Applications and Systems, 2008. BTAS 2008. 2nd IEEE International Conference on, pp.1-6, 2008.

[20] V. D. Kaushik, A. Budhwar, A. Dubey, R. Agrawal, S. Gupta, V. K. Pathak, P. Gupta, An Efficient 3D Face Recognition Algorithm, New Technologies, Mobility and Security (NTMS), 2009 3rd International Conference on, pp.1-5, 2009.